Assessing Operational Total Lightning Visualization Products – Preliminary Results

Geoffrey T. Stano[1*], Christopher B. Darden[2], David J. Nadler[2]

[1]ENSCO Inc. / Short-term Prediction Research and Transition (SPoRT), Huntsville, Alabama
[2]National Weather Service, Huntsville, Alabama

ABSTRACT

In May 2003, NASA's Short-term Prediction Research and Transition (SPoRT) program successfully provided total lightning data from the North Alabama Lightning Mapping Array (NALMA) to the National Weather Service (NWS) office in Huntsville, Alabama. The major accomplishment was providing the observations in real-time to the NWS in the native Advanced Weather Interactive Processing System (AWIPS) decision support system. Within days, the NALMA data were used to issue a tornado warning initiating seven years of ongoing support to the NWS' severe weather and situational awareness operations. With this success, SPoRT now provides real-time NALMA data to five forecast offices as well as working to transition data from total lightning networks at Kennedy Space Center and the White Sands Missile Range to the surrounding NWS offices.

The only NALMA product that has been transitioned to SPoRT's partner NWS offices is the source density product, available at a 2 km resolution in 2 min intervals. However, discussions with users of total lightning data from other networks have shown that other products are available, ranging from spatial and temporal variations of the source density product to the creation of a flash extent density. SPoRT and the Huntsville, Alabama NWS are evaluating the utility of these variations as this has not been addressed since the initial transition in 2003. This preliminary analysis will focus on what products will best support the operational warning decision process. Data from 19 April 2009 are analyzed. On this day, severe thunderstorms formed ahead of an approaching cold front. Widespread severe weather was observed, primarily south of the Tennessee River with multiple, weak tornadoes, numerous severe hail reports, and wind. This preliminary analysis is the first step in evaluation which product(s) are best suited for operations. The ultimate goal is selecting a single product for use with all total lightning networks to streamline training and science sharing.

1. INTRODUCTION

The collaborations between the National Weather Service (NWS) in Huntsville, Alabama and the Short-term Prediction Research and Transition (SPoRT, Goodman et al. 2004; Lapenta et al. 2004) program at the NASA Marshall Space Flight Center have provided unique opportunities for science sharing as well as technology transfer. The SPoRT program's main objective is to facilitate the use of real-time NASA data on the regional and local scale for short time periods (0-24 hours) for operational forecast use (Darden et al. 2002). This partnership, which started with the Huntsville Weather Forecast Office (WFO) now extends to 12 additional WFO partners utilizing data from the Aqua and Terra satellites, partner organizations, and total lightning networks.

*Corresponding author address: Geoffrey Stano, 320 Sparkman Dr, Huntsville, AL 35805
email: geoffrey.stano@nasa.gov

First transitioned to the Huntsville WFO in May 2003, the North Alabama Lightning Mapping Array (NALMA; Goodman et al. 2005) is based on the Lightning Mapping Array developed at New Mexico Tech (Rison et al. 1999). The NALMA is a principle component within a regional severe weather test bed utilizing innovative science and technologies for short-term predictions of hazardous and severe weather (Goodman et al. 2003). With the initial and ongoing success (Bridenstine et al. 2005; Goodman et al. 2005; Darden et al. 2010), the NALMA data have been transitioned to several nearby NWS offices to employ "total lightning" in the warning decision making process. All NWS offices currently receive cloud-to-ground lightning data from Vaisala's National Lightning Detection Network (NLDN). However, the NALMA provides both cloud-to-ground and intra-cloud lightning information, which is often much greater in amount than NLDN activity alone (Boccippio et al. 2001). Initial investigations at the Huntsville WFO and other offices with total lightning data (Sharp 2005) have shown distinct

correlations between the time rate of change of total lightning and trends in the intensity and severity of the parent convective cell. This rate of change also is called a lightning jump (Schultz et al. 2009; Gatlin and Goodman 2010).

The first successful integration of total lightning data with an NWS occurred in the mid-90s at WFO Melbourne, Florida (Starr et al. 1998). The collaborative access to the Lightning Detection and Ranging (LDAR) network, courtesy of NASA's Kennedy Space Center offered the opportunity to investigate the electrical character of severe Florida thunderstorms in real-time (Williams et al. 1999). However, the data were displayed in a system external to the NWS' decision support system AWIPS (Advanced Weather Information Processing System) workstations. This made it difficult to use the data in tandem with radar or satellite. Additionally, unlike the product now provided by SPoRT, the LDAR display shows the raw data with no color-coded method to determine how much activity is occurring at a given location.

As the SPoRT program prepares to provide LDAR information in AWIPS for WFO Melbourne, the question has arisen as to what is the best product for visualization? SPoRT's partners with access to other total lightning networks beyond the NALMA use various combinations of temporal and spatial resolutions for flash extent and source densities. There has been no concerted effort to determine if there is a "best" product for visualization. This paper attempts to address this question. The benefits of determining a "best" visualization product is a unified tool to be used by all WFOs with access to total lightning that will streamline training and science sharing activities among SPoRT's partners. Currently, SPoRT transitions a 2 km resolution source density product that updates every 2 min.

To address this question, a single, preliminary case utilizing NALMA data has been selected. The event from 19-20 April 2009 had severe thunderstorms ahead of an approaching cold front that produced numerous severe hail and wind damage reports along with seven tornadoes. Three broad product categories have been tested. These include source, flash extent, and flash origin densities. Each product category has four variants using different temporal and spatial resolution combinations. Lastly, these combinations are examined within the NWS' decision support system, the Advanced Weather Interactive Processing System (AWIPS).

2. Methodology

The Huntsville WFO selected two case study days for this project, although the preliminary analysis focuses on 19-20 April 2009. The events were specifically chosen as they included multiple severe weather reports that ranged from significant winds to weak tornadoes. Additionally, both events moved completely through the NALMA domain (Figure 1), affording opportunities to investigate the change in detection efficiency with range for each product being tested. The thunderstorms ranged from weak severe storms to supercells.

The first event took place in the evening of 19-20 April 2009 as severe thunderstorms developed ahead of an approaching cold front. Widespread severe weather was observed, primarily south of the Tennessee River, with multiple weak tornadoes, hail, and wind. The second event occurred in the evening of 15-16 June 2009. Here several supercells developed which produced very large hail and significant wind damage.

With the events selected, the NALMA data could be processed. The NALMA, as previously stated, is based on the lightning mapping array developed at New Mexico Tech. The network consists of 11 VHF receivers deployed across north-central Alabama. The network is centered on the National Space Science and Technology Center (NSSTC) on the University of Alabama in Huntsville campus. Each receiver records the time and magnitude of the peak lightning radiation signal received in successive 80 μs intervals, which are then related to the base station at the NSSTC. Due to the volume of data and the need for real-time processing, the data are decimated from 80 μs to 500 μs. These data are then processed to determine the three-dimensional and temporal locations for each source. These sources are what are used to create the source density products and are best considered "pieces of a lightning flash." A single lightning flash may consist of many hundreds of sources, which allows the NALMA to map the spatial and temporal extent of each flash. The NALMA detects sources of both cloud-to-ground and intra-cloud lightning (i.e., total lightning). The detection efficiency decreases with distance from the network center. The effective three-dimensional network

radius is 150 km, while the two-dimensional radius is 250 km.

For SPoRT's partners, these source data are binned onto a 2 by 2 km grid with a 1 km vertical resolution every 120 s. This source density grid is then provided to the NWS with only a 30 s latency from the time of ingest. This is the NALMA's greatest asset as the 120 s time scale is at least half the time of the Weather Surveillance Radar 1998 Doppler (WSR-88D) volume scan updates. This allows forecasters to investigate a storm's intensity in between radar volume scans. For this project, four source density products are created from the raw, real-time observations. These include source densities at resolutions of 1 min by 1 km (currently used by WFO Sterling, Virginia), 1 min by 2 km, 2 min by 1 km, and SPoRT's current product of 2 min by 2 km. These will be abbreviated as sdA, sdB, sdC, and sdD, respectively. A sample, four-panel image is shown in Figure 2.

In addition to the source density products, flash extent and flash origin densities have been created from the raw NALMA data. The flash extent density (Figure 3) is a gridded product that "lights up" a grid cell whenever a flash extends through that grid. A single grid can only be "lit up" by a single flash once, no matter how many sources compose the flash. However, multiple grid boxes can be activated by a single flash. The flash origin density creates a gridded product that only plots the initiation point of individual flashes. The vast majority of flash initiations will be found near the main updraft of the thunderstorm. WFO Houston is currently using a flash extent density for the Houston LDAR. The major difference between the flash extent and flash origin densities, when compared to the source densities, is that the flash densities are created by recombining the raw sources back into flashes by means of a flash creation algorithm. The flash extent densities use the same resolutions as the source densities and are abbreviated as follows: 1 min by 1 km (feA), 1 min by 2 km (feB), 2 min by 1 km (feC), and 2 min by 2 km (feD).

The use of a flash algorithm has two consequences. The positive consequence is the creation of a product that is more intuitive to the end user. A flash extent density of 21 literally means 21 flashes occurred within this grid box for the given time interval. This is similarly true for a flash origin of 12, which means 12 flashes initiated in this grid box. A source density literally means the number of sources, or pieces of a lightning flash, that occurred in the grid box. A source density of 60 means 60 sources were observed in the grid box, but it does not mean 60 flashes were observed. Depending on the flash, 60 sources may correspond to a single flash comprised of 60 sources, ten flashes with six sources each, or some other combination. Therefore, a forecaster cannot correlate a source density to an exact flash density. However, operationally, the more sources observed indicates a stronger storm, much like a high flash extent density would.

For training purposes, a flash extent or origin density is desired due to the intuitive nature of the product. However, there is a drawback to using recombined flashes. No flash creation algorithm is perfect and to be used in real-time it must make very rapid calculations. This causes errors during high flash-rate events as an algorithm may mis-classify the number of actual flashes by combining several small flashes into one flash or breaking a single large flash into several smaller ones. Multiple flash algorithms are available and while each has its own particular strengths and weaknesses, no one algorithm is any better than another in these high flash rate environments (Murphy 2006). With this in mind, we used the flash algorithm described in McCaul et al. (2009) due to its rapid processing of sources into flashes, reflecting the real-time nature of the flash products.

Several issues will be addressed to determine which total lightning visualization product is most useful in an operational setting. The most simple visualizes the various products in AWIPS four-panel displays, as shown in Figures 2 and 3. Additionally, time series plots of each product leading up to a specific severe weather event will be produced. This will be used to qualitatively inspect the trends of total lightning activity in each product. Lastly, the lightning jump algorithm described in Schultz et al. (2009) and Gatlin and Goodman (2010) will be applied to each product to determine if one product or another provides a more effective trending tool.

3. Results

a. The Flash Origin Density

From the beginning, there was concern about the use of the flash origin density product. The concern was that the flash origin density

was essentially a gridded bin of point data. This provides less information than compared to the flash extent and source density products. Unlike those products, a forecaster cannot use the flash origin density to ascertain the spatial extent of lightning. This takes away one of the primary advantages of using total lightning data.

Compounding the issue is that the number of flashes displayed will always be less than the number of sources, since it takes many sources to create a single flash. Also, unlike the flash extent where a single flash may be counted in multiple grid boxes, the flash origin only affects one grid box. This creates a problem within AWIPS which automatically smoothes the data. This smoothing is particularly acute for the 1 min or 1 km variants and also is an issue for the flash extent and source density products. The result is an overly smoothed product that poorly represents total lightning activity. As a result, the flash origin density was dropped as a viable product.

b. Visual Inspection

Each of the four flash extent and source density variants were displayed in AWIPS four-panel displays for ease of comparison (Figure 2 and 3, respectively). This allowed the comparison to be done in the forecaster's native decision support system. In each image the upper left panel is the 1 min by 1 km variant. Then, going clockwise the products are 1 min by 2 km, 2 min by 2 km, and 2 min by 1 km.

Two items are immediately apparent. For the flash extent products, the color curve had to be adjusted to better show the gradient of flash activity since the values are much smaller than the corresponding source density products at the same time. The more serious issue is with the variants that use a 1 km resolution (feA, feC, sdA, and sdC). Compared to the 2 km resolution products, the 1 km resolution products cover 4 times less area, resulting in smaller values being displayed. The auto-smoothing performed by AWIPS immediately lessens the visual impact of these products. This can be offset with improved color curves. However, as can be seen in both Figures 2 and 3, particularly A and C, the spatial extent of the observed lightning is less. It is particularly obvious in the 1 min by 1 km product (feA and sdA). At many times, the feA and sdA appear more like noise than total lightning observations. This reduces the significance of the data and the likelihood of catching a forecaster's attention, particularly when compared to the feD or sdD.

Conversely, the 2 km variants looked less noisy and stood out more when a rapid increase in total lightning occurred. Additionally, the spatial extent of lightning is clearer, greatly helping a forecaster assess the threat posed by potential cloud-to-ground strikes. The 2 min by 2 km data (feD and sdD) variants had the best visual appearance, although the 1 min by 2 km variants (feB and sdB) are a good trade-off of high temporal resolution without suffering from the auto-smoothing of AWIPS.

c. Total Lightning Trends

After the simple visual inspection, a time series of total lightning values for each product variant was produced. Currently, these visualizations for lightning trends are not available in real-time, but efforts are underway to fix this. Looking at these time series in a post event analysis still provides a good investigative tool to further analyze the real-time data. These trends provide further insight into the ramping up of lightning activity and which product best captured the trends.

Figure 4 shows the entire lifetime of a persistent storm that began in northeastern Mississippi and finally decayed near Huntsville, in north central Alabama. As it crossed Alabama, this storm produced six severe hail events, two severe wind events, and five tornadoes. Four tornadoes were classified as EF-0s and the fifth was an EF-1. The flash extent densities are solid lines while the source densities are dashed.

This figure is most useful to compare the two product types in a broad sense than focusing on specific events. It is interesting to note how the flash and source products vary as the storm moves east with time and closer to the center of the NALMA network in Huntsville, Alabama. The flash extent densities appear fairly consistent with time, in part due to the difference in scale with the source density values. An interesting break point can be seen near 2230 UTC as the storm moves within 85 km of the center of the NALMA network. At this point the source density products, particularly sdB and sdD, rapidly increase in value with numerous large peaks starting by 2247 UTC. Meanwhile, the flash extent densities remain more consistent, rarely exceeding 50 flashes.

This highlights an interesting advantage of the flash extent products.

The flash algorithm does not need to have every source that makes up each flash. As a result, at long ranges from the center of the NALMA network when the source detection is lowest, the individual lightning flashes can still be constructed. The overall flash detection efficiency suffers less deterioration compared to that of the sources. As the storms approach the high detection efficiency heart of the NALMA network, the number of sources dramatically increases. The only effect on the flash algorithm is including more flashes per source. The result is a product that does not require a forecaster to pay as much attention to where the storm is located in relation to the center of the network.

While the changes in detection efficiency are superior for the flash products, we need to determine if this translates into a better product. Figures 5 (flash extent density) and 6 (source density) focus on the first two severe hail events in Franklin County just as the storm entered Alabama. The hail was reported at 2206 (5.1 cm) and 2211 UTC (7 cm).

The flash image (Figure 5) shows that the flash extent density trends are not highly pronounced, with the 1 min by 1 km (feA) indicating a subtle increase (3-8 flashes), while the 2 min by 2 km has a more pronounced increase in time with a spike of nearly 10 flashes per 2 min between 2158 and 2200 UTC. All four flash extents indicate a spike in activity just as the first hail event begins.

The source density trends (Figure 6) are in the lower detection efficiency region of the NALMA, but still yield valuable information. Unlike the flash extent products that have a cleaner trend, the source density products look noisier, although the jumps in lightning activity are more pronounced. Both 2 km products (sdB and sdD) consistently observe higher values and clearer increases, although this is partly expected by having a grid box four times larger than the 1 km products (sdA and sdC). The 2 km products indicate an increasing amount of activity nearly 20 min before the first hail event giving the most lead time. The 2 min by 1 km product (sdC) has a smoother appearance and all four source densities show a proportionally large increase at the time of the first hail report.

With this initial inspection of the first 90 min of the storm the 2 km source density products (sdB and sdD) have the most distinct jumps in lightning activity. The flash extent products do indicate increased flash activity and even have proportionally larger percent increases than sdB and sdD. However, discussions with forecasters have indicated that the larger range of values in the 2 km source density products is visually more attention grabbing. Even with a modified color curve, forecaster's confidence in the increase in lightning activity measured in just a few flashes is not enough to issue a warning. This concern is increased when it is remembered that the flashes are recreated by an algorithm that may not always correctly reconstruct the flashes.

The comparison is more interesting for the next hour between 2230 – 2330 UTC in Figures 7 (flashes) and 8 (sources). For this time period, the storm was completely within the good observation range of the NALMA. In this hour an EF-0 (2303) and EF-1 (2318) occurred. Also, severe hail starting at 1.9 cm and increasing to 2.5 cm occurred at 2319, 2323, and 2329 UTC, respectively. Lastly a severe wind report also occurred at 2329 UTC.

The flash products (Figure 7) all indicate a steady ramp up in lightning flashes from 2230 to 2256 UTC, before showing a classic drop-off in activity before the EF-0 at 2303 UTC. The 2 min by 2 km flash extent (feD) had the most obvious increase, while feA was less intense and showed more variability in time due to its 1 min temporal resolution. Following the EF-0, only feD demonstrated a jump in activity starting at 2314 UTC before the other severe weather events. The other three flash extent products only showed a general increase in activity.

The source density products (Figure 8) had more variability than the flash extent counterparts. Again the sdD product has the greatest values and jumps, as is expected with the larger grid box area and 2 min time interval. Still, the sdB indicates two legitimate jumps ahead of the EF-0 at 2303. Meanwhile, sdC has a general increase in activity and sdA would have been of little use for this hour, except for the general increase between 2230 and 2248 UTC. After the EF-0, sdA remains almost constant, except for a jump at 2327 before the severe weather at 2329.

Comparing the two product types, feD was the most consistent as this observed a clear increase by 2316 just prior to the EF-1, while the two best source density products, sdB and sdD

only began to jump right at the time of touchdown. However, radar observations in between the EF-0 at 2303 and the EF-1 at 2318 clearly indicated the storm was maintaining intensity after the initial lightning jumps. Thus, even though sdB and sdD were slower to ramp up again compared to feD, forecasters were already aware of the threat due to the initial jump in feD, sdB, and sdD. Each source density product observed a rapid increase in activity at 2326 UTC prior to the severe weather at 2329 and 2343 (discussed below). The flash extent density products, except feD, did not have this obvious increase ahead of the severe weather, although a general increase is observed.

The final plots occur from 2330 UTC to 0010 UTC on 20 April 2009. During this 40 min period the storm continued on its east-northeastward trajectory and was only 40 to 10 km away from the heart of the NALMA network. An EF-0 touched down at 2343, 4.4 cm hail occurred at 2355, followed by an EF-0 at 2358, and a severe wind report at 2359. The comparison of the two product types dramatically shows the high detection efficiency of the NALMA at this close range.

Figure 9 shows the flash products for the final 40 min of the storm on 19 April 2009. Unlike the previous two time periods (Figures 5 and 7), all four flash products show distinct jumps with each severe weather event. The primary difference is the magnitude. While all four flash variants observed distinct jumps, the warnings required forecaster skill as the jumps were only a few minutes before each severe weather event.

Lastly, Figure 10 has the corresponding source density products. Like the flash products, all four source products clearly jumped before the tornado touchdown at 2343 UTC. Unlike the flash products, the source products jumped to the two highest values observed for the entire event. The sdB and sdD products nearly doubled the next largest observation and were obviously in the midst of another jump ahead of the severe weather that began at 2355 UTC.

At this close range to the center of the NALMA network, practically every product variant successfully jumped for the severe weather events, although the jumps only preceded the severe weather by a few minutes. Percentage-wise, the flash extent density jumps were larger than the source density jumps which are typified by the massive range of values. Feedback from forecasters has indicated that their use of the NALMA product relies more on the range of value increase than percentage of increase. These results, however, have indicated that a percentage increase product may be of value, although this will require a real-time cell tracker.

d. Lightning Jump Algorithm

The previous three sub-sections were mainly qualitative in their analysis of the four variants of flash extent and source density. This qualitative assessment is good as it can quickly assess the visualization of the data in both a plane view and in a time series chart. However, we wanted a more quantitative assessment as well. To this end, we applied the methods described in Schultz et al. (2009) to calculate the lightning jump algorithm on each product variant. The Schultz et al. (2009) paper builds off the initial work by Gatlin (2006) and now published in Gatlin and Goodman (2010). As pointed out in that paper, the jump algorithm is most appropriate for a flash-based product, which will favor the flash extent variants. However, the overall process will provide more quantitative results and has been applied to the source density products as well.

The Schultz et al. (2009), based on Gatlin (2006) method starts by calculating the average flash rate over a 2 min period:

$$FR_{avg}(t_i) = [FR_{t1}(t_1) + FR_{t2}(t_2)] / 2 \qquad (1)$$

$FR_{t1}(t)$ and $FR_{t2}(t)$ are the 1 min total lightning counts from a thunderstorm, and FR_{avg} (flashes per minute) is the 1 min averaged flash rate calculated ever 2 min. Once a period of 10 min had been established for the storm the trend in total flash rate at the next time step can be calculated (DFRDT).

Using the five most recent average flash rates, covering ten minutes, an average of the DFRDT was calculated. In addition to this, the standard deviation, σ, was calculated. For a lightning jump to occur, the current DFRDT value had to exceed the 2σ threshold of the running mean.

For the verification, we indicated that a storm should have a generic severe warning for 30 min from the time of the jump. If any severe weather event occurred within this 30 minute window triggered by a lightning jump, the jump

would be verified. For this project each event was treated separately.

The results are analyzed with contingency tables. The probability of detection (POD), false alarm rate (FAR), and critical success index (CSI) are calculated for each of the eight products being evaluated (Wilkes 1995, 238-241). Additionally, the Heidke skill score (HSS) is calculated, which is better suited to account for rare events. The results of these statistics are summarized in Table 1 (flash extent density) and Table 2 (source density). It is very important to note that this is a preliminary analysis for only 12 events. As a result, the statistical calculations may be skewed heavily due to the small sample size. More storms are being added for future work.

The statistical results are interesting, even when considering the very small sample size. The best PODs came with the sdC and sdD products at 0.92 followed closely by the feC product at 0.91. Surprisingly, the feD only had a 0.73 POD, but the sdA product that did not have good trends as shown in Figures 6, 8, and 10 had a POD of 0.81. Conversely, when focusing on the FAR sdC and sdD had the highest rate at 0.15, while the sdA product scored a zero. A more telling result were the Heidke skill scores, which better accounts for the rare nature of a lightning jump with respect to the entire case. The three best POD scores (feC, sdC, and sdD) also had the best Heidke skill scores of 0.56. It should be noted that the sdA product had a nearly identical Heidke skill score of 0.55 with a POD of 0.81.

The two most interesting results are the high scores for the 1 min by 1 km source density (sdA) and the relatively low scores for the 2 min by 2 km flash extent density (feD), particularly since the feC did as well as it did. Part of the discrepancy is likely due to the very small sample size. When looking at the times for the 12 severe weather events, they are clustered into five groups. This allowed for a single lightning jump to cause multiple verifications. The sdA only needed four jumps to have a POD of 0.81. In fact, few jumps were observed by any of the product types as seen by the low FAR scores that are much less than those observed by Schultz et al. (2009). The low scores for feD are representative of the other flash extent densities, except for feC. Few jumps were registered by these flash products, and the feA only registered a single jump.

These results do appear to underscore the fact that the higher temporal and spatial resolution products do have greater increases in value by percent, but have a poor visualization ability, as seen in Figures 5-10. This is supported by the top three products having 2 min temporal resolutions. As for sdA, while impressive for this small sample set, the ability to visualize these jumps is difficult. Overall, this simple analysis indicates that feC, sdC, and sdD are the most effective products for use.

4. Conclusions

For this preliminary case, a long-tracked storm was observed by the North Alabama Lightning Mapping Array as it tracked east-northeastward from the Alabama-Mississippi border and eventually decayed at nearly the center of the network in Huntsville, Alabama. The total observation time went from 2107 UTC on 19 April 2009 to 0010 UTC on 20 April. During this time, four tornadoes, six hail, and two wind events occurred.

The purpose of this project was to evaluate which total lightning product may be best for use in the National Weather Service's operations. Currently, the SPoRT program provides a 2 min by 2 km source density product, but other total lightning users have variations ranging from 1 min by 1 km to flash extent densities. Efforts here to find the most useful product will help standardize total lightning use and training.

Initially three product types were considered; flash extent, flash origin, and source densities. Immediately, the flash origin density was discounted as the relatively small values were heavily smoothed by the NWS' AWIPS display, making the product look more like noise than lightning data. Additionally, using only the flash origin removed one of total lightning's greatest strengths; being able to observe the spatial extent of lightning.

Based on the limitations of the flash origin density, our project constrained its focus to the flash extent and source density products. Each product type had four temporal and spatial variants. These variants were 1 min by 1 km (feA and sdA), 1 min by 2 km (feB and sdB), 2 min by 1 km (feC and sdC), and 2 min by 2 km (feD and sdD).

Each product and variant has its own strengths and weaknesses. The 1 min resolution products are highly desired for the ability to observe changes within a thunderstorm

at sub-radar volume scan times. The flash products are more intuitive to train with as everyone understands “a flash” as compared to what “a source” is. In addition, the flash extent products have superior detection efficiency at the edges of the NALMA domain. The drawback to the flash products is that the flash products require a flash creation algorithm to reconstruct the flashes from the raw source data. This makes the flash extent density only as good as the algorithm making the flashes, which may reconstruct the flashes improperly. The primary advantage of the source density products is that these are the raw data. Except for the calculations to determine the three dimensional location of each individual source, there are no further calculations necessary. This removes uncertainty as to the accuracy of the observations when secondary calculations, such as the flash algorithm, are applied to the data. The drawback is that training is more difficult and the detection efficiency of sources improves quickly as the storm approaches the center of the network.

Visually, the 1 min and 1 km products suffered the most in AWIPS (Figures 2 and 3). Due to the nature of the way information is ingested and visualized in the AWIPS system, total lightning data tends to be smoothed considerably. As a result the higher temporal and spatial resolution products were often smoothed too much. This was due to the inherently smaller values that would occur in the smaller grid boxes or with a smaller observation time window. This smoothing was particularly bad for the 1 km products and, to a lesser extent, all of the flash extent products. The flash extents, being reconstructed from the raw sources, always had smaller values. This smoothing problem consistently made these products appear more like noise than actual observations. This was less of a problem near the center of the network and for the 2 min by 2 km flash extent (feD). Additionally, the sdB was one of the best 1 min resolution products as it used a 2 km resolution and sources.

When comparing the products using a time series of observations, three products were the most consistent in providing valuable observations. These were the feD, sdB, and sdD. The feD flash product was the only flash product selected as the other flash variants usually only showed broad increases in lightning activity before severe weather or the actual range in the values during the increase was small. By percent increase, the flash products usually showed larger increases than the source products. This percent increase was very difficult for forecasters to discern if the range was on the order of 10 flashes. Conversely, the source products had increases of 100 sources or more that were visually far easier to observe and thus gain the forecaster’s attention. The source density products did suffer from artificial increases in observations due to improving detection efficiency as the storm approached the center of the NALMA. However, this bias is a longer-scale trend, requiring tens of minutes to occur. An actual lightning jump will occur in less than ten minutes. This artificial increase may have been in effect from 2200 to 2230 UTC (Figure 4, dashed lines), but there were still several large source density increases in this time. Except for a rapidly moving storm, this detection efficiency issue is likely not going to affect the outcome, although forecasters need to be aware of this.

Lastly, the lightning jump algorithm described by Schultz et al. (2009) was applied to all eight product variants. Care should be taken to not place too much weight on the statistical results as the dataset had too few events (12) to make this a fully viable statistical analysis. The top three products had POD scores of 0.91 and 0.92 (feC, sdC, and sdD). Additionally, the Heidke skill score for these three products was 0.56, the highest in our analysis. Surprisingly, and likely due to the small sample set, the 1 min by 1 km source density product (sdA) had a POD of 0.81 and a Heidke skill score of 0.55.

Overall, one product was consistently seen in each of our simple analyses. This was the 2 min by 2 km source density product (sdD). When visually displayed in AWIPS, on a time series plot, or with the jump algorithm the sdD was successful in alerting a forecaster that a storm was intensifying. Due to its spatial and temporal resolution, the sdD was less affected by the smoothing of AWIPS. However, there are drawbacks. First, the 2 min temporal resolution is not as desired as the 1 min products. If data are available at a higher frequency, forecasters want that higher frequency. Also, being a source density product, it is more subject to the effects of the detection efficiency of the NALMA network. As a result, forecasters need to pay attention to how quickly a storm is moving into or out of the NALMA domain, as artificial jumps or decreases are possible. It is likely these artificial changes can be recognized as separate from

true lightning jumps as they occur over tens of minutes as opposed to a true lightning jump on the order of ten or fewer minutes. Another side effect of being a source density is that the training is more difficult as a source density is less intuitive than a flash extent density.

Additional work is clearly necessary before a final conclusion as this preliminary analysis had too few events. With this in mind, the flash extent density products at 2 km (feC and feD) remain viable candidates. Also, future work with AWIPS II, the next generation of decision support systems for the NWS, will not have the same smoothing issue as AWIPS. This may make the 1 min by 1 km products more viable, visually. Still, these 1 min by 1 km products (feA and sdA), have very small ranges in values, hampering their use in a real-time setting. Efforts to implement a lightning jump algorithm in real time may help offset this problem. The 1 min by 2 km source density (sdB) appears to be an interesting compromise product with high temporal resolution, but the courser spatial resolution that allows for a greater range of values and better visualizations. The main issue with this product is the lower skill scores for this initial, small dataset.

Acknowledgements: The authors would like to thank Mr. John Hall for his time in helping produce the variant products for display in AWIPS.

5. Bibliography

Boccippio, D. J., K. L. Cummins, H. J. Christian, and S. J. Goodman, 2001: Combined satellite- and surface-based estimation of the intracloud-cloud-to-ground lightning ratio over the continental United States. *Mon. Wea. Rev.*, **129**, 108-122.

Bridenstine, P. V., C. B. Darden, J. Burks, and S. J. Goodman, 2005: The application of total lightning in the warning decision making process. 1st *Conf. on Meteorological Applications of Lightning Data*, Amer. Meteor. Soc., San Diego, CA, P1.2.

Darden, C. B., D. J. Nadler, B. C. Carcione, G. T. Stano, and D. E. Buechler, 2010: Utilizing total lightning information to diagnose convective trends. *BAMS,* DOI: 10.1175/2009BAMS2808.1

Darden, C., B. Carroll, S. Goodman, G. Jedlovec, B. Lapenta, 2002: Bridging the gap between research and operations in the National Weather Service: Collaborative activities among the Huntsville meteorological community. *NOAA Technical Memorandum,* PB2003-100700, NWS Southern Region, Forth Worth, TX.

Gatlin, P. N. and S. J. Goodman, 2010: A total lightning trending algorithm to identify severe thunderstorms. *J. Atmos. Oceanic Tech.*, **27**, 3-22.

Gatlin, P. N., 2006: Severe weather precursors in the lightning activity of Tennessee Valley thunderstorms. M.S. thesis, The University of Alabama in Huntsville, 87 pp.

Goodman, S. J., R. Blakeslee, H. Christian, W. Koshak, J. Bailey, J. Hall, E. McCaul, D. Buechler, C. Darden, J. Burks, T. Bradshaw, and P. Gatlin, 2005: The North Alabama Lightning Mapping Array: Recent severe storm observations and future prospects. *Atmos. Res.*, **76**, 423-437.

Goodman, S. J., W. M. Lapenta, G. J. Jedlovec, J. C. Dodge, and J. T. Bradshaw, 2004: The NASA Short-term Prediction Research and Transition (SPoRT) Center: A collaborative model for accelerating research into operations. *20th Conf. on Interactive Information Processing Systems (IIPS) for Meteorology, Oceanography, and Hydrology*, Amer. Meteor. Soc., Seattle, WA, P1.34.

Goodman, S. J., R. Blakeslee, H. Christian, W. Koshak, J. Bailey, J. Hall, E. McCaul, D. Buechler, C. Darden, J. Burks, and T. Bradshaw, 2003: The North Alabama Lightning Mapping Array: Recent results and future prospects. *12th Int. Conf. on Atmosphere Electricity*, Versailles, France, June 2003.

Lapenta, W. M., R. Wohlman, T. Bradshaw, G. Jedlovec, S. Goodman, C. Darden, J. Burks, and P. Meyer, 2004: Transition from research to operations: Assessing value of experimental forecast products within the NWSFO environment. *16th Conf. on Numerical Weather Prediction*, AMS, Seattle, WA, January 2004.

McCaul, E. W., S. J. Goodman, K. M. LaCasse, and D. J. Cecil, 2009: Forecasting lightning threat using cloud-resolving model simulations. *Wea. Forecasting*, **24**, 709-729.

Murphy, M. J., 2006: When flash algorithms go bad. *1st Intl. Lightning Meteorology Conf.*, Tucson, AZ, 26-27 April 2006.

Rison, W., R. J. Thomas, P. R. Krehbiel, T. Hamlin, and J. Harlan, 1999: A GPS-based three-dimensional lightning mapping system: Initial observations in central New Mexico. *Geophys. Res. Lett.*, **26**, 3573-3576.

Schultz, C. J., W. A. Petersen, and L. D. Carey, 2009: Preliminary development and evaluation of lightning jump algorithms for the real-time detection of severe weather. *J. Appl. Meteor. Clim.*, **48**, 2543-2563.

Sharp, D. W., 2005: Operational applications of lightning data at WFO Melbourn, FL: A 15-year retrospective. *1st Conf. on Meteorological Applications of Lightning Data,* Amer. Meteor. Soc., San Diego, CA.

Starr, S., D. Sharp, J. Madura, F. Merceret, and M. Murphy, 1998: LDAR, a three-dimensional lightning warning system: It's development and use by the government and transition to public availability. *35th Space Congress*. Cocoa Beach, FL.

Wilkes, D. S., 1995: *Statistical Methods in the Atmospheric Sciences*. Academic Press, 467 pp.

Williams, E. R., B. Boldi, A. Matlin, M. Weber, S. Hodanish, D. Sharp, S. Goodman, R. Raghavan, and D. Buechler, 1999: The behavior of total ightning activity in severe Florida Thunderstorms. *Atmos. Res.*, **51**, 245-265.

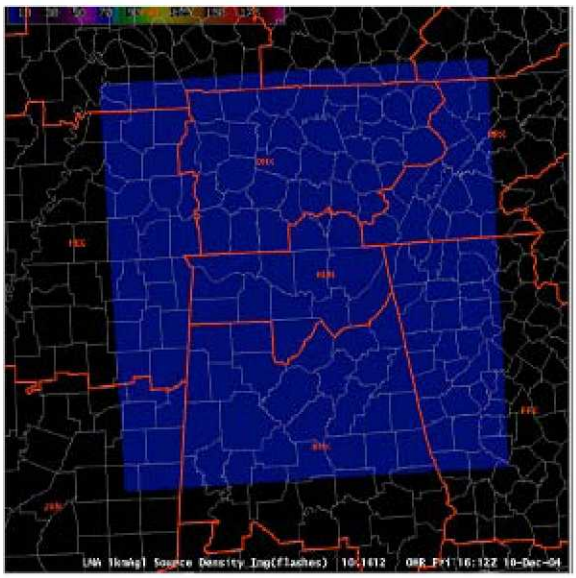

Figure 1: The blue shaded area shows the North Alabama Lightning Mapping Array domain within AWIPS. The WFO county warning areas are outlined in red, with WFO Huntsville in the center.

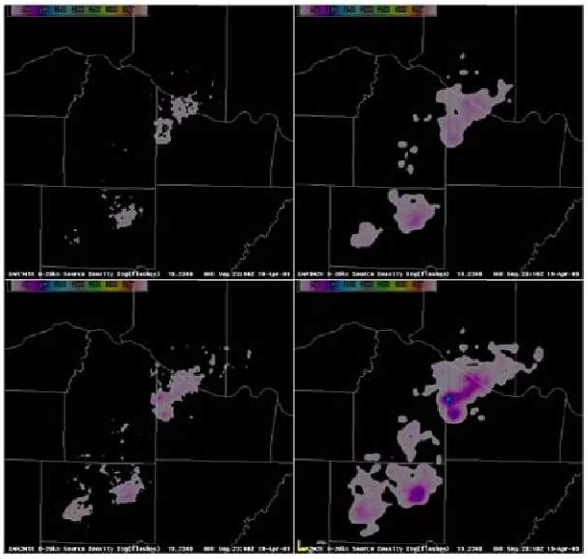

Figure 2: An AWIPS four panel display of total lightning source density product variants at 2340 UTC on 19 April 2009. These include 1 min by 1 km (upper left, sdA), 1 min by 2 km (upper right, sdB), 2 min by 1 km (lower left, sdC), and 2 min by 2 km (lower right, sdD).

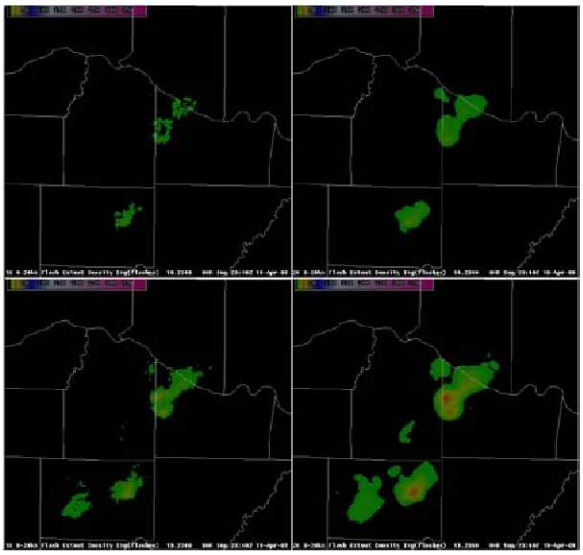

Figure 3: This is the same as Figure 2, but displaying flash extent densities. The color curve has been altered to better visualize the smaller values in the flash extent density products compared to the source density products. These are 1 min by 1 km (upper left, feA), 1 min by 2 km (upper right, feB), 2 min by 1 km (lower left, feC), and 2 min by 2 km (lower right, feD).

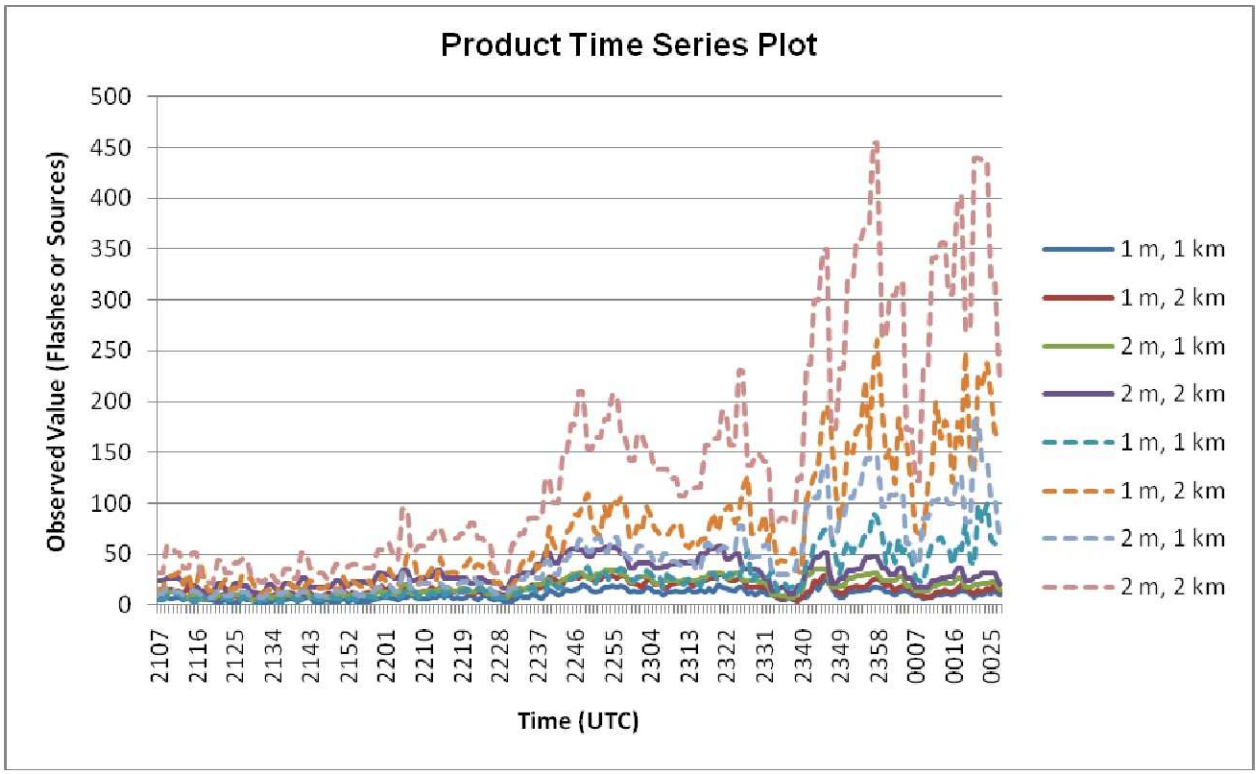

Figure 4: A time series from a single storm moving through the NALMA domain showing the values of the flash extent density product (solid lines) and source density product (dashed lines) from 2107 UTC on 19 April 2009 to 0027 UTC on 20 April 2009.

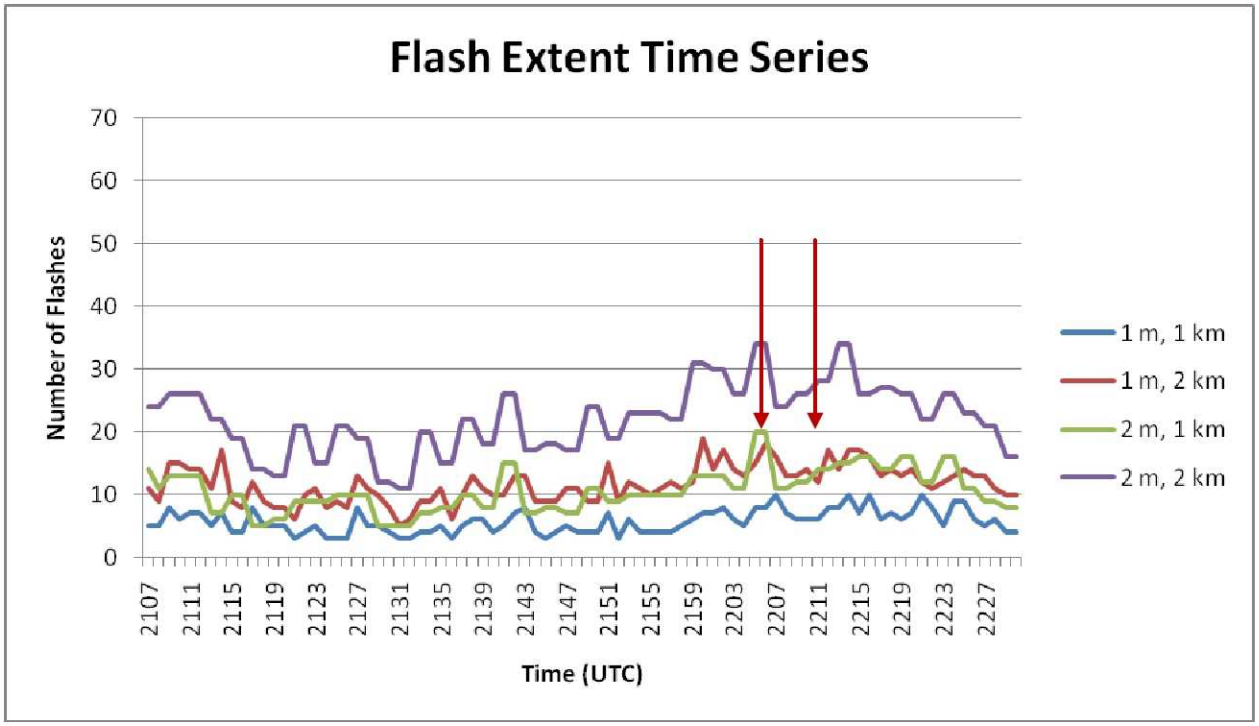

Figure 5: A time series of the four flashe extent products from 2107 to 2230 UTC on 19 April 2009. The severe hail events occurred at 2206 and 2211 UTC and are marked by the red arrows.

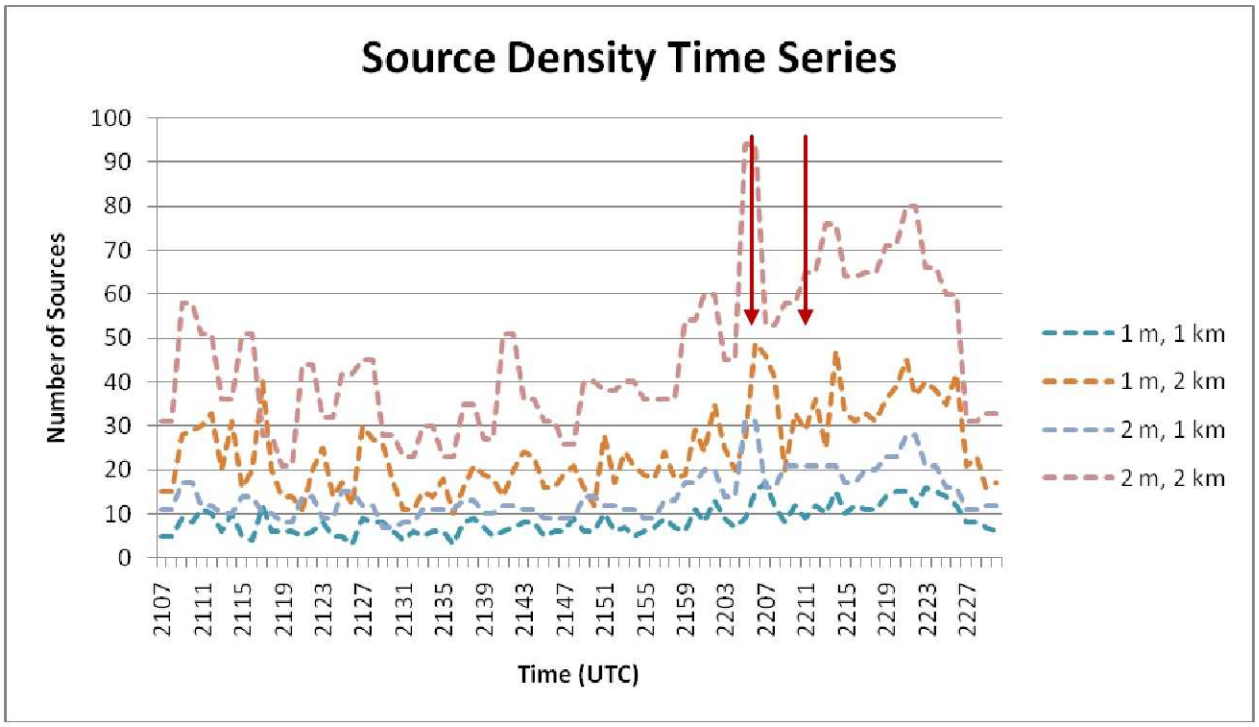

Figure 6: Same as Figure 5 but using the four source density products.

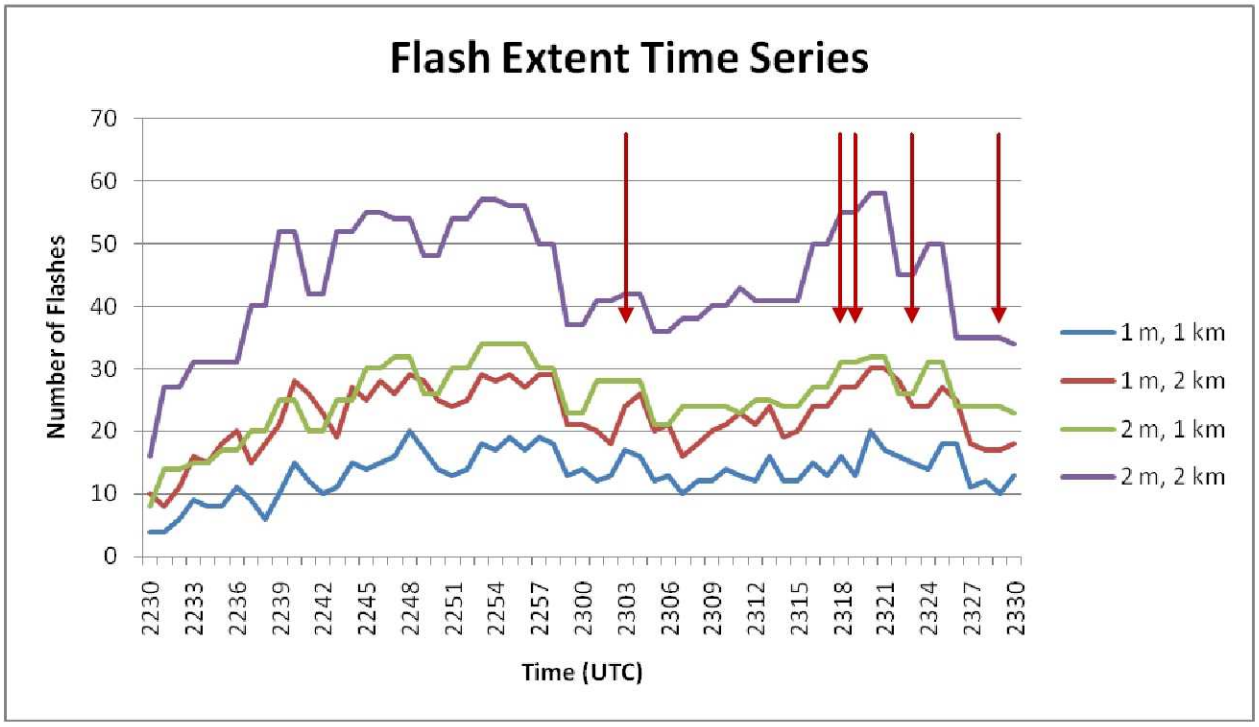

Figure 7: Same as Figure 5 but covering the time period from 2230 to 2330 UTC on 19 April 2009.

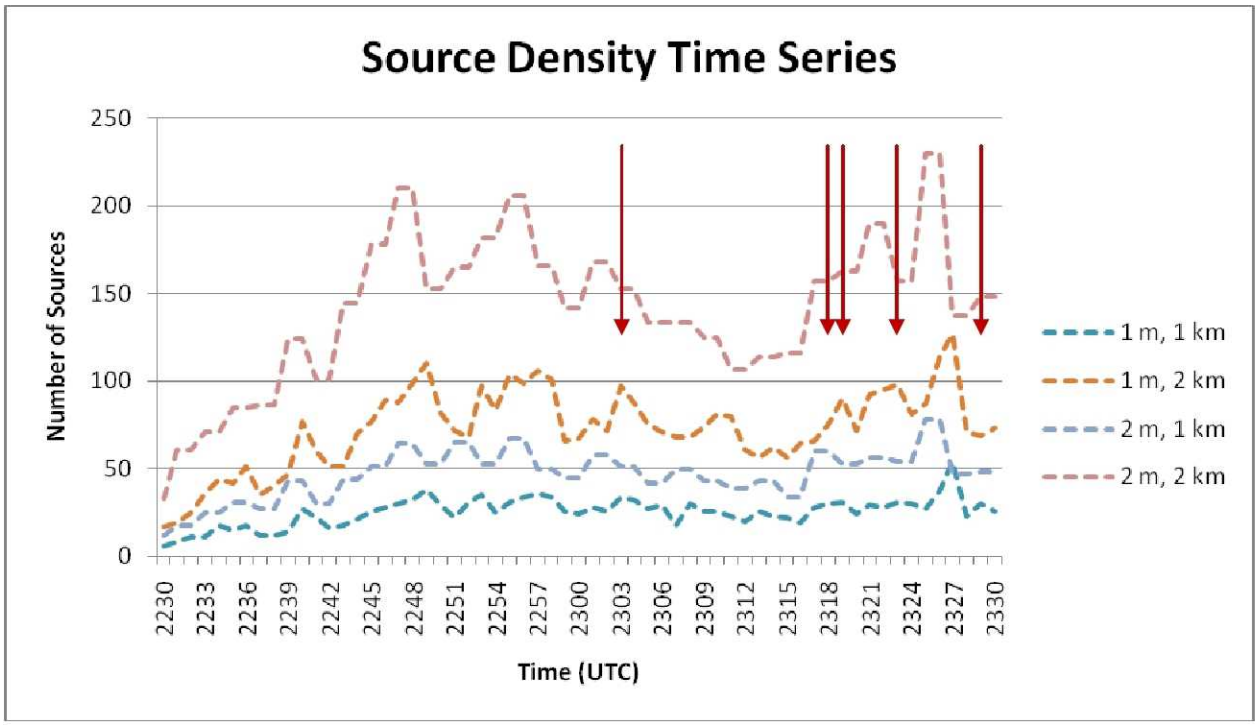

Figure 8: Same as Figure 7 but for the source density products.

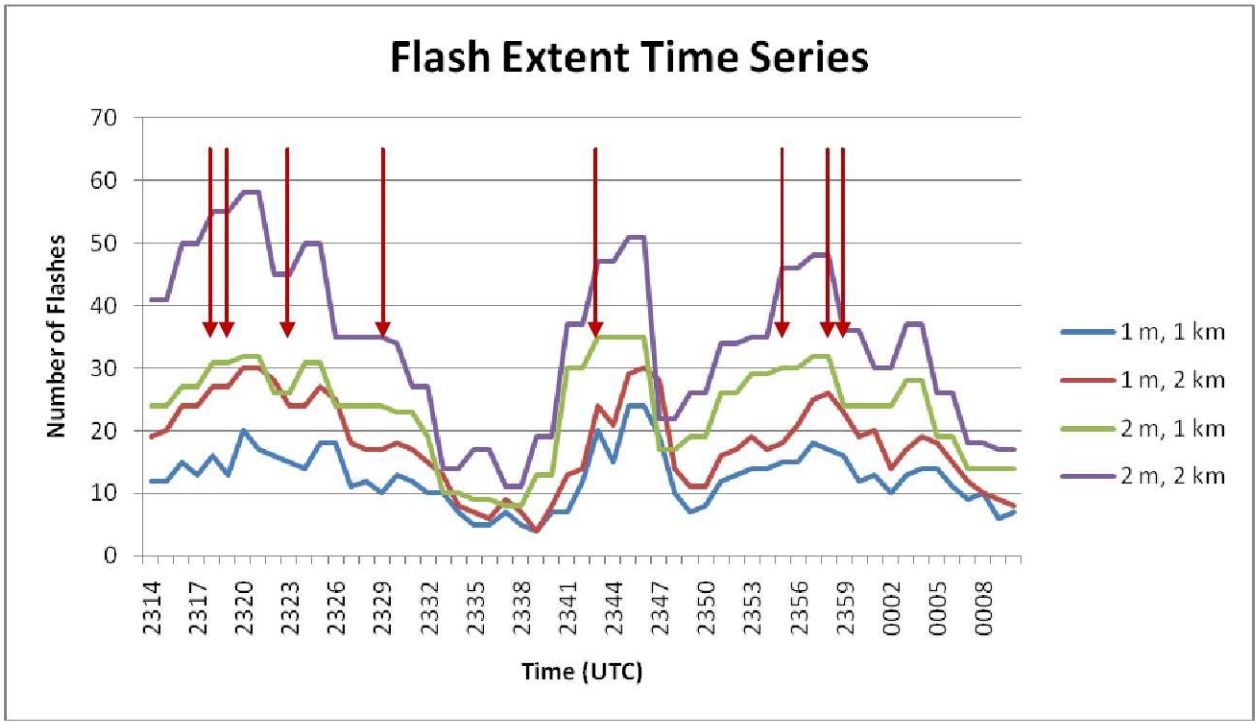

Figure 9: Same as Figure 5 but covering the time period of 2314 UTC on 19 April, 2009 to 0010 UTC on 20 April, 2009.

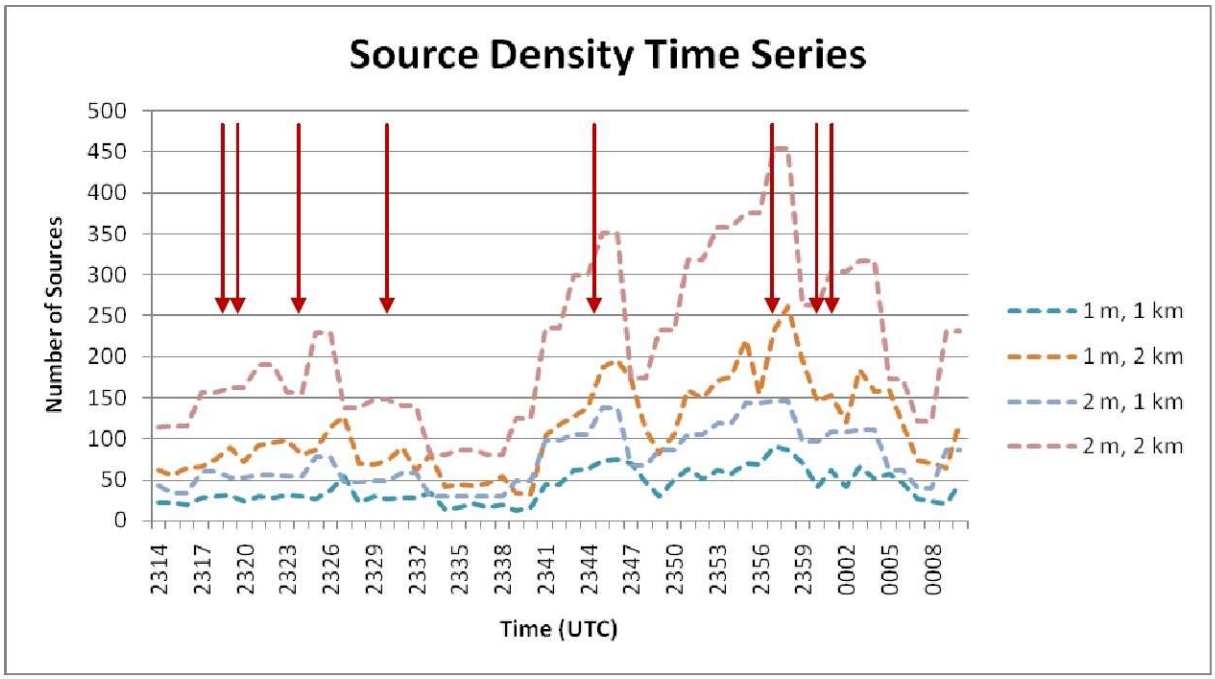

Figure 10: Same as Figure 9 but for the source density products. Note that for this period, the number of sources scale is double that of Figures 6 and 8.

Table 1: Statistical scores for the four flash extent density products for the event covering 19 April 2009.

Flash Extent	1 min by 1 km	1 min by 2 km	2 min by 1 km	2 min by 2 km
Probabilty of Detection	0.27	0.54	0.91	0.73
False Alarm Rate	0	0.14	0.09	0.11
Critical Success Index	0.27	0.5	0.83	0.67
Heidke Skill Score	0.43	0.48	0.56	0.52

Table 2: Statistical scores for the four source density products for the event covering 19 April 2009.

Source Density	1 min by 1 km	1 min by 2 km	2 min by 1 km	2 min by 2 km
Probabilty of Detection	0.81	0.54	0.92	0.92
False Alarm Rate	0	0.14	0.15	0.15
Critical Success Index	0.81	0.5	0.78	0.78
Heidke Skill Score	0.55	0.48	0.56	0.56